Available online at www.sciencedirect.com
SCIENCE DIRECT®
Biochemical Pharmacology 68 (2004) 1971–1984
Biochemical Pharmacology
www.elsevier.com/locate/biochempharm

Photoreceptor preservation in the S334ter model of retinitis pigmentosa by a novel estradiol analog

James A. Dykens[a,*], Amy K. Carroll[a], Sandra Wiley[a], Douglas F. Covey[b], Zu Yun Cai[b], Lian Zhao[c], Rong Wen[c]

[a]*MitoKor Inc., 11494 Sorrento Valley Road, San Diego, CA 92121, USA*
[b]*Department of Molecular Biology and Pharmacology, Washington University School of Medicine, St. Louis, MO 63110, USA*
[c]*Department of Ophthalmology, University of Pennsylvania School of Medicine, Philadelphia, PA 19104, USA*

Received 16 February 2004; accepted 15 June 2004

Abstract

The cytoprotective activity of MITO-4565, a novel, non-hormonal, estradiol derivative, was evaluated in the S334ter transgenic model of retinitis pigmentosa (RP). Progressive blindness in RP is due to apoptotic death of the photoreceptors, a process mimicked by the animal models [Portera-Cailliau C, Sung C-H, Nathans J, Adler R. Apoptotic photorecepter cell death in mouse models of retinitis pigmentosa. Proc Natl Acad Sci USA 1994;91:974–8]. On postnatal day 9, 10 transgenic S334ter rats received a single intraocular injection of MITO-4565 in the left eye, and vehicle in the right eye. By postnatal day 20, the thickness of the outer nuclear layer (ONL) in the superior retina of the untreated eyes was 5.76 ± 1.12 μm (N = 10), versus 10.72 ± 1.52 μm (N = 10) for eyes treated with MITO-4565 ($P < 0.0001$, ANOVA F = 1671). Comparable cytoprotection was also observed for the inferior retina. Cytoprotection by MITO-4565 was also observed in primary cultures of rat retinal ganglion cells against NMDA excitotoxicity. Data from studies of hexose monophosphate shunt flux, mitochondrial stability, and in vitro lipid peroxidation, are in accord with previous reports [Green PS, Gridley KE, Simpkins JW. Nuclear estrogen receptor independent neuroprotection by estratrienes: a novel interaction with glutathione. Neuroscience 1997;84:7–10]; a likely mechanism of action entails moderation of membrane lipid peroxidation in a redox couple with glutathione. Such preservation of membrane integrity is particularly crucial to mitochondria, where collapse of membrane potential precipitates cell death, and where GSH is maintained at mM concentrations. Indeed, exposure to MITO-4565, but not a methoxy substituted negative control, allowed mitochondria to retain membrane potential ($\Delta\Psi_m$) under conditions of Ca^{2+} overload that would normally induce complete mitochondrial failure. Mitochondrial interventions offer a novel therapeutic approach for RP, and other degenerative diseases of the retina.

Keywords: Mitochondria; Glutathione; Lipid peroxidation; Retinal ganglion cells; Apoptosis

1. Introduction

Retinitis pigmentosa is a heterogeneous collection of inherited syndromes characterized by progressive blindness that results from the apoptotic death of retinal photoreceptors [1]. At least 150 mutations have been linked to retinal degeneration in RP, with a preponderance found in photoreceptor-specific proteins, including rhodopsin [3–5], peripherin [6–8], the β subunit of the cGMP phosphodiesterase [9–11], and a rod outer segment protein, ROM-1 [12].

Important for etiological validation, introduction of selected rhodopsin mutations into the genomes of mouse [13], rat [14], and pig [15], yields a progressive apoptotic loss of rods and cones comparable to the human disease phenotype, albeit occurring more rapidly in the animal models. For example, in the transgenic rat model used here, the human rhodopsin mutation S334ter induces swift photoreceptor degeneration, with 50% of the photoreceptors succumbing over a single 48 h interval between postnatal days (PD) 11 and 12 [16]. This rapid photoreceptor loss is paralleled by a sharp increase in caspase-3 activation, and intraocular administration of specific caspase-3 inhibitors correspondingly moderates this photoreceptor

Abbreviations: ONL, outer nuclear layer; GSH, glutathione; HMS, hexose monophosphate shunt

* Corresponding author. Tel.: +1 858 509 5617; fax: +1 858 793 7805.
E-mail address: dykensj@mitokor.com (J.A. Dykens).

0006-2952/$ – see front matter © 2004 Elsevier Inc. All rights reserved.
doi:10.1016/j.bcp.2004.06.042

degeneration [16]. The evidence is compelling that the caspase-3-dependent apoptotic cell death pathway is a proximate mediator of photoreceptor death in this, and other models of retinal degeneration [1,17–21].

Mitochondria occupy the nexus of cell death and viability pathways, especially in long-lived energy demanding cells such as neurons (including many retinal cell types), myocardium, pancreatic beta cells, and kidney [22–24]. Although it is increasingly clear that most cells have redundant pathways capable of initiating apoptosis, mitochondrial compromise or failure often triggers apoptosis [25].

When mitochondrial function fails acutely, as occurs when hypoxia conspires with inordinately excessive cytosolic Ca^{2+} to undermine the impermeability of the inner mitochondrial membrane, the cell will die from necrosis as the ATP-demanding ion-dependent transport pumps fail to maintain osmotic equilibrium across the plasma membrane [26–28]. On the other hand, under less severely injurious conditions, mitochondrial integrity, and hence apoptosis, is actively regulated by a family of pro- and anti-apoptotic proteins, including bcl-2, bax, bad, and β-NAC, among others [23,29]. Under pro-apoptotic stimuli, these family members interact, forming a complex assemblage of hetero and homo aggregates that induce mitochondria instability, leading to an irreversible loss of the mitochondrial inner membrane impermeability [22,30]. Such mitochondrial destabilization and failure can also be induced by Ca^{2+} overload, and it is potentiated by free radical exposure, as well as other stressors that directly or indirectly undermine inner mitochondrial membrane integrity [27,31,32]. In addition to the energetic crisis precipitated by the failure of oxidative phosphorylation, mitochondrial collapse is associated with the release of cytochrome *c* and other proteins, typically smaller than 1200 kD, that lead to the activation of downstream effector caspases that systematically dismantle the cell via proteolysis. Of these, caspase-3 activation is generally considered to be a point of no return in the apoptotic cascade [23,33].

The ability of estrogen (17β-estradiol; 17β-E2) to protect neurons, and many other cell types, against a wide variety of noxious stimuli has been widely reported [34]. For example, 17β-E2 variously protects, retinal, hippocampal, amygdalal, cortical, and mesencephalic neurons from serum deprivation, from β-amyloid toxicity, and from oxidative stress [35–42]. Similarly, in animal models, estrogens have been shown to attenuate ischemia-induced retinal degeneration [43], neuronal loss after ischemia in the middle cerebral artery occlusion model, neuronal excitotoxic death in the kainic acid seizure model, and in a contusion physical injury model [44–49].

Until recently, such cytoprotection could be ascribed most parsimoniously to hormonally mediated genomic responses, or to non-genomic signaling mechanisms mediated by non-nuclear estrogen receptors [34,35]. However, in studies using diverse cell types exposed to a variety of stressors, 17α-estradiol (17α-E2), a naturally occurring diastereomer of 17β-E2 that is 200–1000-fold less active as a hormone depending on the tissue, has been found to be equally as cytoprotective as 17β-E2 [34,35,50,51]. These studies and others have fostered a model in which neuroprotection is mediated by non-genomic mechanisms independent of the classical estrogen receptors, and where the minimal structural element required for neuroprotection is identified as the steroid A-ring phenol [34–36,39,50–52].

Mechanistic and structure–activity relationship studies have led to a working hypothesis in which the lipophilic A-ring phenolic steroids intercalate into cell membranes [53] where they terminate lipid peroxidation chain reactions, which can be lethal to retinal neurons [54], becoming a stable radical in the process [55–57]. Experiments in vitro showing a 400-fold increase in potency of these molecules upon addition of reduced glutathione [2,56] have further suggested that the steroidyl radical generated by reduction of the peroxyl within the membrane bilayer is subsequently reduced by glutathione, thereby regenerating the native phenolic steroid and allowing it to repeatedly terminate peroxidations via redox cycling. Such a membrane stabilization mechanism would be particularly germane to mitochondria, where organellar failure, and hence cellular life or death, are determined by the impermeability of the inner membrane and consequent maintenance of the mitochondrial membrane potential ($\Delta\Psi_m$) [57,58].

This hypothetical model makes several testable predictions, namely, (1) that the ability of phenolic steroids to moderate lipid peroxidation in vitro should be augmented by exogenous glutathione, (2) that glutathione utilization via redox cycling should be accelerated by phenolic steroids in vivo, (3) that membrane stabilization by these compounds should be reflected in mitochondrial function and integrity, and (4) that such mitochondrial stabilization should translate into improved cellular resistance to injurious stimuli.

Accordingly, the ability of representative members of a library of novel polycyclic phenolic estrogen analogs to moderate lipid peroxidation was examined in vitro. The molecules under investigation include 17β-estradiol, 17α-estradiol, the enantiomer of 17β-estradiol where the stereochemistry at all the chiral carbons has been reversed thereby making it a mirror image of the parental molecule (*ent*-E2) [51], plus MITO-4565, MITO-4567, and MITO-4555. MITO-4565 is 17β-E2 with a lipophilic electron-donating adamantyl moiety ortho to the A-ring hydroxide [56,59] (Fig. 1), whereas MITO-4567 substitutes a methoxy group for the latter, rendering it inactive as a cytoprotectant both in vitro and in vivo thereby providing a negative control [50] (Fig. 1). MITO-4555 is 17β-E2 with an additional hydroxy at the 6α position of the B-ring [(6α, 17β)-estra-1,3,5 (10)-triene-3,6,17-triol], and is another negative control with no cytoprotection activity apparent in several cell models.

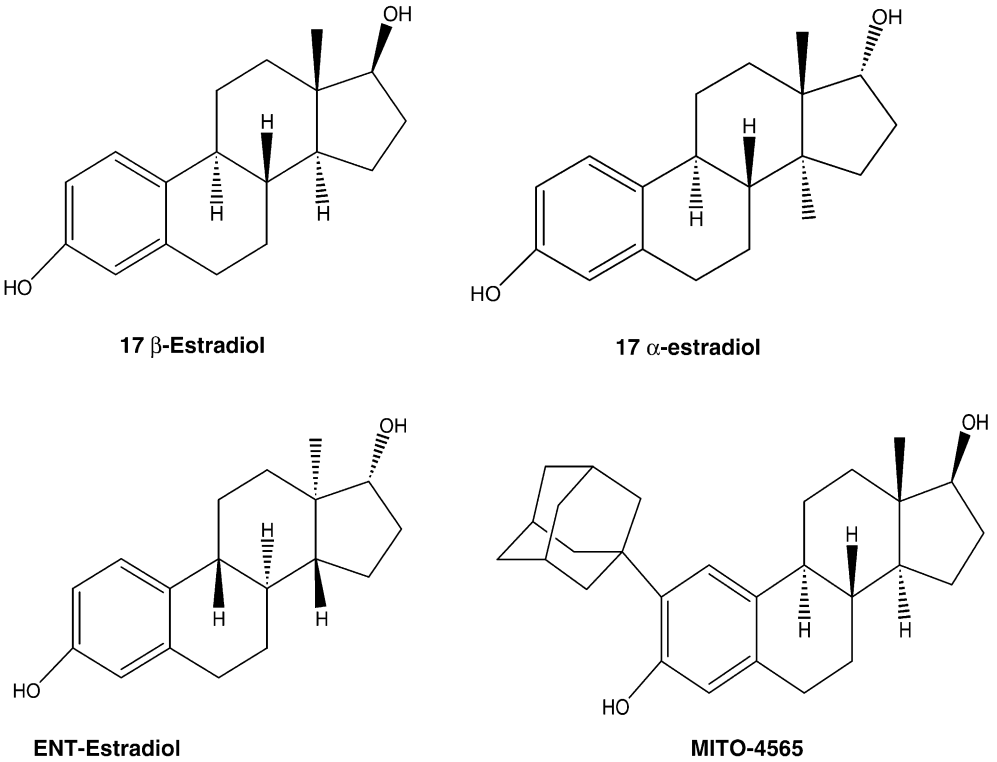

Fig. 1. Polycyclic phenolic analogs of 17β-estradiol. 17β-estradiol is profoundly active as a feminizing hormone, whereas 17α- estradiol, which differs only in the stereochemistry at the 17 position of the D ring, and the enantiomer of 17β-estradiol (*ent*-E2), although chemically indistinguishable from the parental 17β-estradiol, are both hundreds of fold less active as a hormones. MITO-4565 contains an electron donating, lipophilic adamantyl group on the A-ring.

The ability of these compounds to increase glutathione utilization was examined in intact human erythrocytes, where flux through the glycolytic hexose monophosphate shunt provides a direct indication of NADPH turnover and glutathione reductase activity unconfounded by alternate metabolic pathways [60,61]. Similarly, the ability of these compounds to increase mitochondrial tolerance of excessive Ca^{2+} loading was assessed in situ using a fluorescence resonance energy transfer (FRET) assay that reports mitochondrial membrane potential ($\Delta\Psi_m$) [57,62]. The neuroprotective activities of these compounds were assessed in primary cell culture using retro-labeled retinal ganglion cells. Finally, the possibility that MITO-4565, the most active of these compounds in the micelle- and cell-based assays, could correspondingly moderate apoptotic degeneration of photoreceptors in vivo was examined using the S334ter transgenic rat model of RP where apoptotic cell death is dependent on caspase-3 activation [16].

2. Materials and methods

2.1. Chain-breaking antioxidant effects

The ability of these phenolic steroids to act as chain-breaking antioxidants in vitro was assessed using liposomes made from soy bean phosphatidyl choline incubated in the presence of test compound and the lipid-soluble radical initiator 2.2′-azobis(2,4′-dimethylvaleronitrile) (AMVN). Liposomes were prepared from lyophilized powder (Sigma Chemicals), by suspension in chloroform with subsequent evaporation under vacuum and reconstitution with vigorous agitation in liposome buffer (0.1 M NaCl, 1 μM EDTA). This procedure yields mutlilamellar liposomes, which were stored at −80 °C until use. Radical initiator (AMVN) was purchased from Wako Pure Chemical in crystal form and prepared as a 1000× stock in ethanol prior to each experiment.

Thawed liposomes were brought to a final concentration of 10 mg/ml in liposome buffer and incubated with 10 μM compound or vehicle control in a 50 °C water bath. The mixture was gently stirred using a magnetic stir plate. At 30–120 min prior to the addition of AMVN, 20 μl samples were drawn and subjected to HPLC analysis to insure lack of significant, endogenous, peroxide formation in the preparation. Phosphatidyl choline hydroperoxide was separated using a Phenosphere silica column (250 mm × 4.6 mm, 5 μm) (Phenomenex), and 90% MeOH, 10% 40 mM $NaHPO_4$ buffer in the mobile phase. Hydroperoxide was detected by UV-absorbance at 254 nm. Once a baseline level of hydroperoxide formation had been established, AMVN was added to a final concentration of 600 nM. Samples were drawn every 10–30 min and subjected to HPLC as described above. Ability to slow the rate

of peroxide formation was determined by peak height analysis and related to peroxide levels measured in vehicle control samples.

To determine if compounds that act as chain-breaking antioxidants could interact with exogenous glutathione, the above assay was modified slightly. The final concentration of AMVN was increased to 1 μM, compound concentration dropped to 1 μM, and GSH was added to a final concentration of 1 mM.

2.2. Assessment of hexose monophosphate shunt (HMS) flux

In human RBCs virtually all of the reducing potential and ATP are generated via the classical Embden–Meyerhof–Parnas glycolytic pathway, so that HMS flux can be construed as directly reflecting NADPH utilization [61]. RBC HMS flux was determined as previously described [63]. Briefly, blood was obtained via venipuncture from a healthy volunteer, washed three times in Kreb's Ringers containing 5 mM glucose (KRG) using 6 min centrifugation at 1800 × *g* to separate RBS from KRG. The leukocyte buffy coat was removed after each centrifugation. RBCs were resuspended in KRG to 25% vol in KRG, and 3 ml placed into 10 ml Erlenmeyer flasks tightly sealed with a rubber gasket. KOH CO_2 gas trap (100 μl) was suspended in a well above the cells. Test compounds were added, and after 10 min thermal equilibration to 37° in a thermostated shaking water bath, 0.3 μCi of ^{14}C-U-glucose (Amersham Biosciences) was added. Sixty minutes later, metabolism was stopped and CO_2 forced out of solution via injection of 1 ml 10% $HClO_4$ through the sealed gasket. After an additional 5 min equilibration, 10 μl of the KOH was removed from the trap well (=10% of total) and placed into 5 ml scintillation cocktail (Ready Safe, Beckman-Coulter), which was counted using a Beckman LS 6500 counter. Control flasks containing all materials except test compounds, plus blank flasks containing all reactants but where metabolism had been stopped at time 0 via addition of 10% $HClO_4$, were run in parallel.

2.3. Effects on mitochondrial membrane potential ($\Delta\Psi_m$)

Mitochondrial membrane potential was followed in digitonin permeabilized SHSY-5Y neuroblastoma cells using a assay based on fluorescence resonance energy transfer (FRET) between two dyes: nonyl acridine orange (NAO) and tetramethylrhodamine (TMR) [62]. The presence of TMR quenches NAO emission in proportion to $\Delta\Psi_m$, while loss of $\Delta\Psi_m$ with consequent efflux of TMR, dequenches NAO [64].

Neuroblastoma SHSY-5Y cells were obtained from American Type Tissue Collection and propagated in high glucose Dulbecco's modified Eagle's medium. Cells are trypsinized and plated in clear-bottom, black-walled, 96-well plates (Costar 3606, Corning International) at 60,000/well 24 h prior to assay, as described previously [62,64].

Because NAO photobleaches under ambient illumination, a solution is made fresh every 4 h by diluting a frozen stock solution (5.16 mM in ethanol, stored in dark) to 516 nM in warm Hank's balanced salt solution (HBSS). Dilute NAO (20 μl) is added directly to cells in 100 μM culture media to a final concentration of 86 nM. Cells were incubated with NAO for 6 min, after which the media is removed and the cells washed 3× with warm HBSS before being transferred to the plate reader where TMR is added (final concentration 150 nM). TMR is made fresh daily by diluting a frozen stock (40 mM in DMSO) into warm KCl media, detailed below, to a concentration of 750 nM. All dyes are obtained from Molecular Probes. The laser on the Fluorescence Imaging Plate Reader (FLIPR; Molecular Devices) is run at 600 mW. In order to focus on the quenching of NAO, while minimizing signal from TMR, the standard emission filter in FLIPR was replaced with a narrow bandpass filter of 525 ± 6 nm, obtained from Omega Optical. Cells are washed 3× with warm 125 mM KCl containing 1 mM $MgCl_2$, 4 mM each of succinate, glutamate, and malate as oxidizible substrates, 2 mM HEPES, and 1 mM KH_2PO_4 pH 7.0, and then permeabilized with 0.008% digitonin in the FLIPR upon addition of TMR. Tolerance of Ca^{2+} exposure and onset of mitochondrial permeability is assessed by adding serial dilutions of the KCl media containing exogenous Ca^{2+} [62].

2.4. Retinal ganglion cell (RGC) excitotoxicity

RGCs were labeled and cultured using previously described methods [54]. Briefly, ganglion cells were retrogradely labeled by stereotactic injection of 1 μl of the fluorescent tracer 4′-6-diamidino-2-2 phenylindole (DAPI; Molecular Probes) dissolved in dimethylformamide into the superior colliculi of anesthetized postnatal day 2–4 Long-Evans rats. At postnatal day 7–9 the animals were sacrificed by decapitation, the eyes enucleated, and the retinas dissected free in HBSS. After two incubations in HBSS containing papain (12.5 U/ml), each for 30 min at 37°, the retinas were gently triturated with a Pasteur pipette and plated on poly-L-lysine-coated 96-well flat-bottom tissue culture plates at a density of approximately 2000 cells/mm^2. The cells were cultured for 24 h in Eagle's minimal essential medium with methylcellulose (0.7%), glutamine (2 mM), gentamicin (1 μg/ml), glucose (22.5 mM final concentration), and prescreened fetal calf serum 5%).

RGCs viability was determined by loading cells with non-fluorescent calcein-acetoxymethyl ester (calcein–AM), which fluoresces green when cleaved by esterases in living cells. Survival of RGCs was quantified by counting the percentage of DAPI-positive cells that were also calcein positive in three high-power fields using 96 well

plates. Treatments were run in triplicate, and assessed in a blinded format. Results are expressed as mean ± S.E.M., and are compared to control conditions consisting of culture medium alone. In a pre-incubation variation of the experiment, 24 h prior to sacrifice, 2 μl of the compound under scrutiny was injected into the vitreous of both eyes (10 mM solution in DMSO), and the ensuing cultures were correspondingly incubated with test compound prior to NMDA treatment (labeled pre-incubation in Fig. 6).

2.5. Transgenic animal studies

Homozygous breeders of line 3 of transgenic rats that carry a murine rhodopsin mutant S334ter (S334ter-3) were kindly provided by Dr. M.M. LaVail (University of California, San Francisco, CA). Heterozygous S334ter-3 rats were produced by mating homozygous breeders with wild-type Sprague-Dawley rats. All experiments were performed using heterozygous S334ter-3 rats. Controls were age-matched Sprague-Dawley rats. Animals were kept in a 12 h light/dark cycle at an in-cage illuminance of 10 fc (foot-candles) (1 fc = 510.76 lx (lux)). The in-cage temperature was kept at 20–22 °C. Intraocular injections were given directly into the vitreous by 32 gauge needles.

Ten transgenic animals were used for intravitreal injection of MITO-4565. MITO-4565 was dissolved in DMSO (10 mM) and delivered by intravitreal injection through 32 gauge needles. At PD 9, the left eye of an animal was injected with 2 μl of MITO-4565 in DMSO, and the right eye with 2 μl DMSO as a vehicle control. All 10 transgenic animals were sacrificed at PD 20 by CO_2 overdose and eyes were collected and fixed in 2.5% glutaraldehyde and 2% paraformaldehyde. Eyes were embedded in an Epon/Araldite mixture, sectioned to 1 μm thickness to display the entire retina along the vertical meridian [16,65,66]. Retinal sections from both the vehicle-treated and compound-treated eyes were examined by light microscopy and evaluated independently by three experienced scientists. In addition, the thickness of the outer nuclear layer (ONL) in the superior and inferior retina 500 μm from the optic nerve head was measured using a microruler under a 60× oil objective lens. Dosing on PD 9 and examination on PD 20 was done in order to facilitate comparisons with treatments previously evaluated in this model using this same protocol. A second intraocular injection was not well tolerated by the animals. All studies were in compliance with the Association for Research in Vision and Ophthalmology (ARVO) Statement for the Use of Animals in Ophthalmic and Vision Research, and with the Declaration of Helsinki.

2.6. Statistical analyses

Effects on mitochondrial membrane potential were quantified by calculating the area under the curve after Ca^{2+} challenge [62]. To partially correct for variations in cell density, staining, and optical aberrations, the area under the curve post Ca^{2+} addition (AUC) was divided by the amount of initial quenching of NAO [62]. Dose–response data were fitted using non-linear regression analysis (sigmoid models) with GraphPad Prism software, version 3.00 for Windows (GraphPad Software, San Diego, CA, USA). One-way ANOVA analysis and Bonferroni comparisons on HMS data and ONL thickness were done with the same software.

3. Results

Induction of peroxidation via AMVN autoxidation (600 nM) yields linear rates of peroxide formation, as shown by upper control regression (Fig. 2). Pre-incubation of micelles for up to 3 h with MITO-4565 had no effect on peroxide formation prior to AMVN addition, as reflected by flat slopes in both controls and treated micelles (Figs. 2 and 3). However, upon addition of 600 nM AMVN, 10 μM MITO-4565 significantly moderates lipid peroxidation compared to controls ($P < 0.01$ at all times after 15 min), and continues to do so for up to 2 h, when the experiment ended. Comparable moderation of peroxide formation is apparent with 17β-E2 (Fig. 3A), although absolute rates of peroxide formation differ from Fig. 2 because liposome concentrations differed between experiments.

Addition of GSH to the media qualitatively alters the response, postponing the onset of peroxide formation and maintaining it at a slower rate compared to controls, at least until 150 min at which time the regressions begin to converge (Fig. 3B). By using a higher concentration of

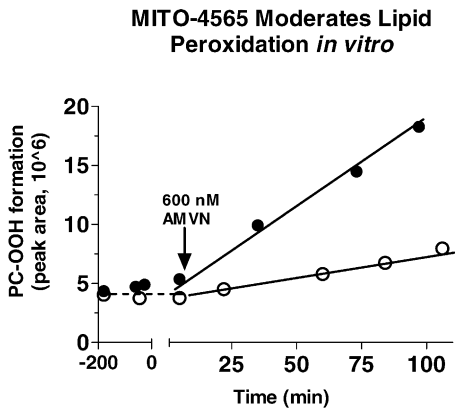

Fig. 2. MITO-4565 moderates lipid hydroperoxide formation. Using multilamellar liposomes made from soy bean phosphatidyl choline incubated in the presence of test compound (10 μM) and the lipid-soluble radical initiator 2.2′-azobis(2,4′-dimethylvaleronitrile) (AMVN) at 600 nM. Hydroperoxide formation is minimal prior to AMVN exposure (added at time 0), and it increases linearly for at least 90 min (closed circles; linear regression $r^2 = 0.997$). MITO-4565, added at the start of the 30 min pre-incubation period, significantly reduces the rate of hydroperoxide formation (open circles), with the linear regression having a significantly lower slope = 0.043 ± 0.003 S.E. ($N = 3$; $r^2 = 0.986$; $P < 0.001$ covariance analysis) vs. 0.137 ± 0.005 ($N = 3$) for untreated controls.

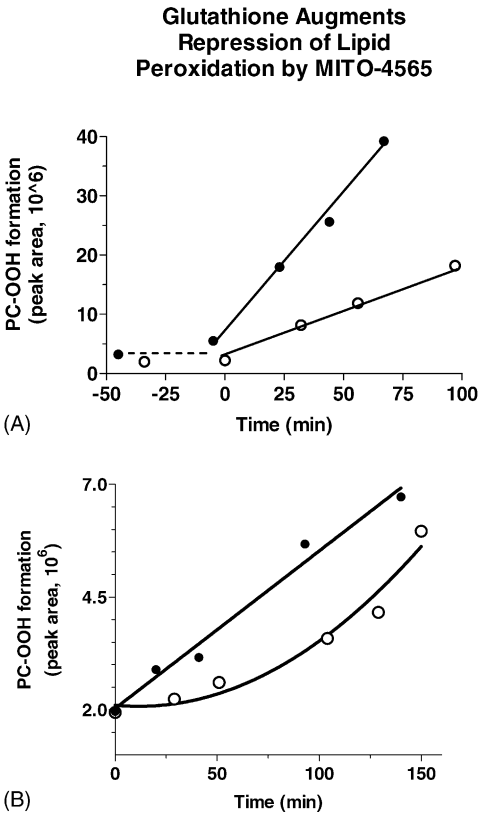

Fig. 3. Moderation of lipid peroxidation is augmented by exogenous reduced glutathione (GSH). As in Fig. 2 hydroperoxide formation is moderated by MITO-4565 compared to untreated control liposomes (panel A). Addition of 1 mM GSH to the incubation media, a concentration 5–10-fold lower than what is maintained in mitochondria in vivo, qualitatively alters the kinetics of peroxidation, inducing a lag period, and further repressing peroxidation rates, at least for 130 min (panel B). It should be noted that direct comparisons between panels A and B are tenuous because 17β-E2 was present at 1 μM, and peroxidation was induced with 1 μM AMVN in panel B, vs. 10 μM and 600 nM, respectively, in panel A.

AMVN, which increases the molar amount of radicals produced, and simultaneously dropping the concentration of test compound, the chain-breaking activity of the compounds could no longer overcome propagation of lipid peroxidation, i.e., the ability of the test compound to slow hydroperoxide formation became indistinguishable from that of the vehicle control. This helped to insure that any change in rate of peroxide formation upon addition of glutathione to the aqueous phase was due to interactions between the test compound and exogenous GSH. Glutathione (1 mM) added to the assay in the absence of test compound, had no effect on peroxide formation, not surprising given that AMVN generates radicals within the lipid membrane while GSH is a hydrophilic antioxidant. The inability to moderate hydroperoxide formation by the two negative control compounds lacking cytoprotective activity is shown in Table 1.

Human erythrocytes (RBCs) lack a nucleus and mitochondria, relying solely on classical glycolytic metabolism for both ATP and reducing potential. They therefore provide an extremely simple system in which to assess HMS

Table 1
Inhibition of lipid peroxidation by steroid analogs after 30 min exposure to AMVN

Compound	% Inhibition of peroxidation no GSH (mean ± S.E.)	% Inhibition of peroxidation plus 1 mM GSH (mean ± S.E.)
17β-E2	40.6 ± 12.5	57.4 ± 8.6
MITO-4565	52.8 ± 15.5	69 ± 7.4
MITO-4555	−4.9 ± 3.2	None detected
MITO-4567	5.2 ± 4.2	None detected

Detection of lipid hydroperoxides following 30 min incubation with the lipophilic radical generator AMVN (600 nM), plus the indicated compounds at 10 μM (detailed in Section 2). Rates (means ± S.E., $N = 6$) have been normalized as percent untreated control.

flux and NADPH turnover without the confounding generation or utilization of reducing equivalents or CO_2 via alternate pathways [61]. Monitoring glucose flux through the hexose monophosphate shunt in human erythrocytes indicates that the compounds alone have no effect (Fig. 4A). However, upon addition of 10 mM H_2O_2, HMS flux significantly increases (Fig. 4B), a response that is differentially augmented by 1 μM 17β-E2, 17α-E2, *ent*-E2, and MITO-4565, but not by MITO-4567, the negative control (Fig. 4B).

Similar responses are also detected at the level of mitochondrial membrane potential ($\Delta\Psi_m$) using a FRET assay that relies of interactions between nonylacridine orange (NAO), a mitochondria-specific cardiolipin stain, and tetramethylrhodamine (TMR), a Nernstian potentiometric dye [64]. Control mitochondria treated with buffer plus vehicle, and those incubated for 10 min with MITO-4567, show comparable intolerance of an imposed Ca^{2+} load, with collapse of $\Delta\Psi_m$ readily apparent at an EC_{50} 23–24 μM Ca^{2+} (Fig. 5). However, 10 min incubation with the cytoprotective compounds effectively increases Ca^{2+} tolerance by an average of 28%, with treated mitochondria retaining $\Delta\Psi_m$ at intermediate Ca^{2+} concentrations sufficient to induce almost complete $\Delta\Psi_m$ collapse in untreated mitochondria (Fig. 5). This increased mitochondrial stability is apparent in the EC_{50} values which represent the Ca^{2+} concentration required to reduce $\Delta\Psi_m$ by 50%: control = 24.0 ± 1.8 μM; MITO-4567 = 23.0 ± 2.6 μM; 17β-E2 = 32.4 ± 0.9 μM; *ent*-E2 = 31.6. ± 3.0 μM; 17α-E2 = 30.5 ± 1.3 μM; MITO-4565 = 36.5 ± 1.1 μM. Thus, compared to untreated or negative control samples, within intermediate Ca^{2+} concentrations, mitochondria treated with cytoprotective compounds tolerated higher levels of Ca^{2+} before failing.

Assessment of retinal ganglion cell (RGC) cytoprotection was performed using two formats: (1) test compound and NMDA were added simultaneously, (2) compound was injected into the vitreous 24 h prior to sacrifice, and was present in culture media prior to NMDA exposure (pre-incubation). NMDA kills between 30 and 60% of the RGCs within 24 h (Fig. 6A and B) and both 17β-estradiol (MITO-139), and to a lesser extent 17α-estradiol

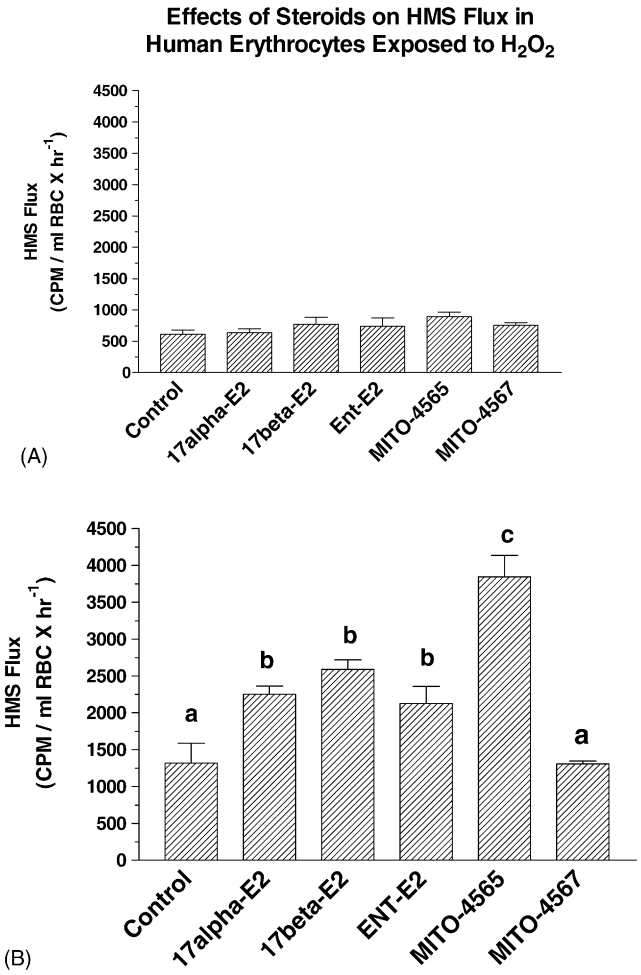

Fig. 4. Carbon flux through the hexose monophosphate shunt in normal human erythrocytes (red blood cells; RBCs). In the absence of an oxidative insult, the compounds have no effect on HMS flux (panel A). However, exposure to 10 mM H_2O_2 significantly increases HMS flux in untreated control RBCs (panel B). Treatment with the indicated compounds at 1 μM for 10 min prior to addition of 0.3 μCi ^{14}C-U-glucose results in varying increases in HMS flux, with 17β-E2, 17α-E2, and *ent*-E2 all showing comparable responses. MITO-4565 significantly increased HMS flux over the estradiols, and MITO-4567, a non-cytoprotective negative control, yields HMS flux rates indistinguishable from untreated controls. Means not significantly different at $P < 0.05$ (Bonferroni), share superscripts; ANOVA $F = 22.18$, $P < 0.0001$. Background flasks containing all reactants plus addition of 10% $HClO_4$ at the start of the experiment were included to control for spontaneous glucose hydrolysis (data not shown).

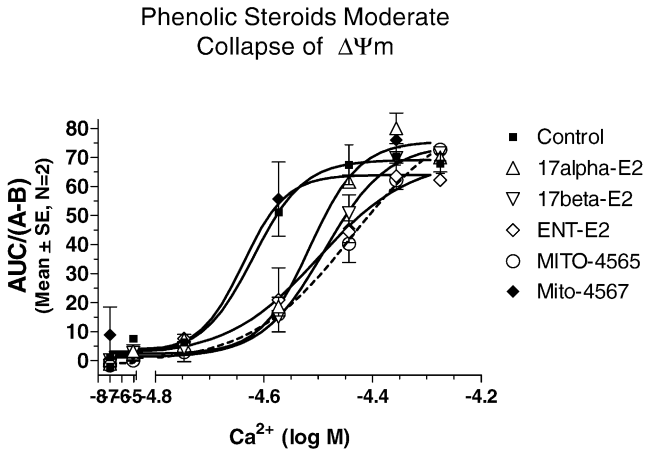

Fig. 5. Cytoprotective compounds preserve mitochondrial membrane potential ($\Delta\Psi_m$) during pathogenic Ca^{2+} exposures. $\Delta\Psi_m$ was monitored in situ using a fluorescence resonance energy transfer (FRET) assay. Acute exposure to Ca^{2+} concentrations ranging from 0 to 50 μM induces varying degrees of $\Delta\Psi_m$ collapse in digitonin-permeabilized SHSY-5Y neuroblastoma cells. In vehicle treated cells (control) or in cells treated with MITO-4567, a non-cytoprotective negative control, $\Delta\Psi_m$ collapse is nearly complete at 25 μM Ca^{2+} (solid symbols). Conversely, cells treated with the indicated estradiols at 0.5 μM for 10 min prior to Ca^{2+} challenge retained $\Delta\Psi_m$, as reflected by the right shift in the dose–response curves. Of the compounds evaluated, MITO-4565 was the most effective MITO-protective agent, which is also reflected by the EC_{50} values presented in Section 3.

(MITO-4509), significantly protected RGS with pre-incubation (Fig. 6A), but not when added at the same time as NMDA (Fig. 6B). Regardless of the experimental format, MITO-4565 exerted significant cytoprotection of RGCs against excitotoxicity, whereas the negative control compound, MITO-4567, failed to do so (Fig. 6A and B).

The progressive photoreceptor degeneration in the retinas of heterozygous S334ter-3 rats follows a pattern as described by Liu et al. [16]. In virtually all animals, degeneration is evident as early as postnatal day (PD) 8 and by PD 20, more than 90% photoreceptors are lost in all the animals. Fig. 7 shows a representative section of the superior retina from wild-type (panel A) and S334ter-3 animals (panel B) at PD 20. In wild-type Sprague-Dawley rats, the outer nuclear layer of the retina contained 11–12 rows of photoreceptor nuclei and the inner and outer segments were well developed (Fig. 7A). Severe degeneration was observed in vehicle treated eyes of all 10 treated transgenic animals. Shown in Fig. 7B is a section of the superior retina from the right eye of a S334ter-3 rat that received a single injection of DMSO vehicle at PD 9. Only 1–2 rows of nuclei remain in the ONL, and very short inner segments with no visible outer segments. In the left eye of this animal, which was treated with a single intravitreal injection of MITO-4565 in DMSO at PD 9, the retina retained 2–4 rows of nuclei in the ONL, and the inner segments were better preserved (Fig. 7C). To quantify this response, the thickness of the outer nuclear layer (ONL) in the superior and inferior retina was measured 500 μm from the optic nerve head, using a microruler under a 60× oil objective lens. In vehicle treated eyes, the ONL thickness in superior retina was 5.76 ± 1.12 μm (mean ± S.D., n = 10) and 8.32 ± 1.65 μm (n = 10) in the inferior (Fig. 8). In contrast, ONL thickness in the contralateral eye treated with MITO-4565 was 10.72 ± 1.52 μm (superior retina, n = 10) and 15.84 ± 2.06 μm (inferior retina, n = 10). Both superior and inferior domains in the eyes exposed to MITO-4565 are significantly greater than the vehicle treated counterparts ($P < 0.0001$, one-way ANOVA, $F = 1100$ for superior; $P < 0.0001$, $F = 696$ for inferior) (Fig. 8). To underscore how extensive the retinal degeneration is in this model, in wild-type animals at PD 20, the ONL thickness

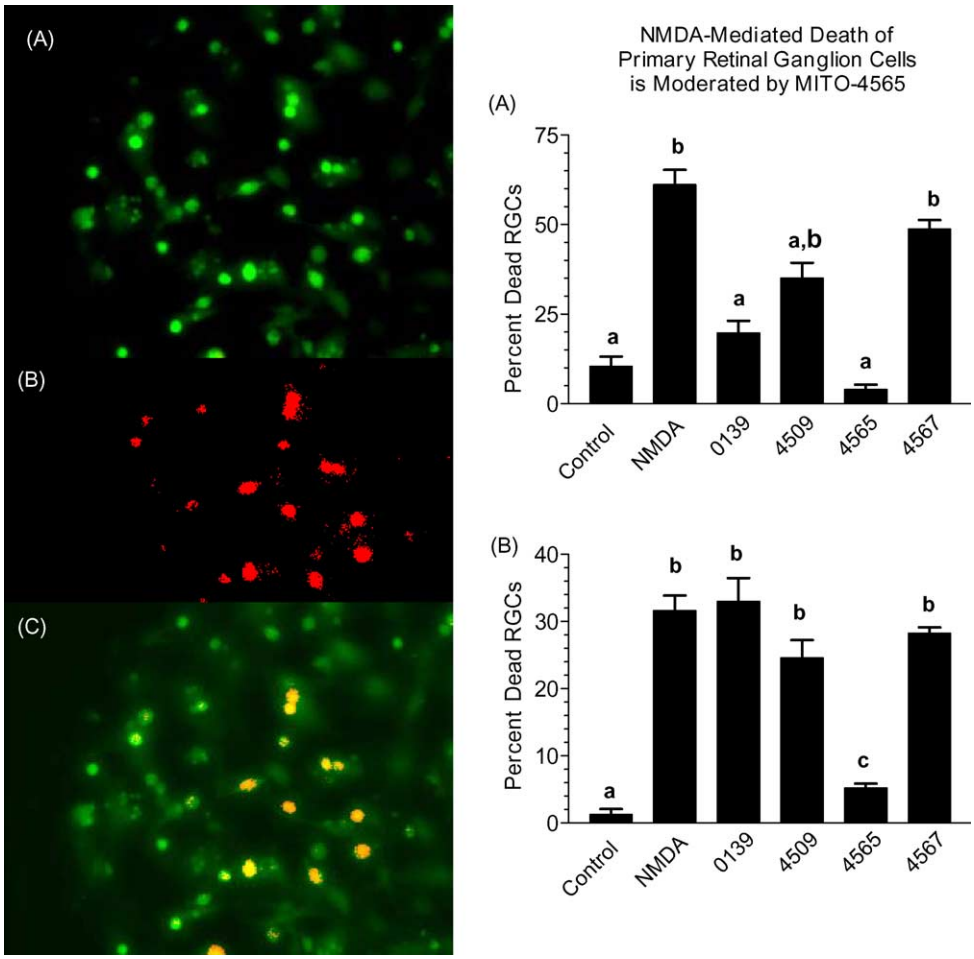

Fig. 6. MITO-4565 protects retinal ganglion cells (RGCs) in primary culture from excitoxicity. Living RGCs in primary culture fluoresce green after exposure to calcein-AM (panel A), whereas only retrograde labeled DNA of RGCs fluoresces red (panel B). The overlay (panel C) reveals that many of the RGCs fail to fluoresce green, indicating that they are dead, whereas others have both red and green signals, indicating that they are alive. Counting live vs. dead cells indicates that MITO-4565 protects RGCs against NMDA toxicity regardless of whether the animals were pretreated, and cells pre-incubated, with compound (bar graph A) or whether compound was added at time of NMDA exposure (bar graph B). Conversely, 17β-estradiol and 17α-estradiol both require pretreatment to show cytoprotection (Fig. 6 bar graph A). Regardless of experimental format, the negative control failed to provide protection (bar graph inserts). Means not significantly different (Kruskal–Wallis one-way ANOVA and Dunn's multiple comparison) share superscripts. Panel A: ANOVA $F = 39.08$, $P < 0.001$; panel B: ANOVA $F = 42.54$, $P < 0.001$, $N = 9$ per group).

was 40.80 ± 1.70 μm (superior retina, $n = 5$) and 44.16 ± 1.31 μm (inferior retina, $n = 5$) (Fig. 8).

4. Discussion

The cytoprotective activities of hormonally active estrogens have been extensively documented [34,42], but structure–activity studies with a variety of steroidal analogs have increasingly revealed that the molecular motifs required for cytoprotection with this class of compounds differ significantly from the structural requirements for estrogen receptor-dependent gene transcription [2,35,36,39,50–52]. For example, although the enantiomer of 17β-estradiol (*ent*-E2) has identical physiochemical properties as 17β-E2, its affinity at the stereospecific estrogen receptors (ERs) is orders of magnitude lower [67–69]. Despite inactivity as a feminizing hormone in estrogen-responsive tissues, *ent*-E2 exerts neuroprotective effects both in vitro and in vivo that are comparable to authentic 17β-E2 [51]. These studies and others have defined the minimal structural elements required for neuroprotection as a hydroxy on the steroid A-ring and planarity of the steroid ring backbone [39,50–52,70].

Mechanistic studies with these molecules have led to a model where the planar hydrophobic steroid intercalates into cell membrane and there terminates lipid peroxidation chain reactions, becoming a stable radical in the process [55–57]. Experiments in vitro showing a 400-fold increase in potency upon addition of glutathione [1] have further suggested a mechanism where the steroidyl radical is subsequently reduced by glutathione, thereby regenerating the native phenolic steroid, which can then participate in another peroxidation termination cycle. In this way, the phenolic steroid serves as a catalyst, allowing the reducing potential of the metabolically maintained glutathione pool

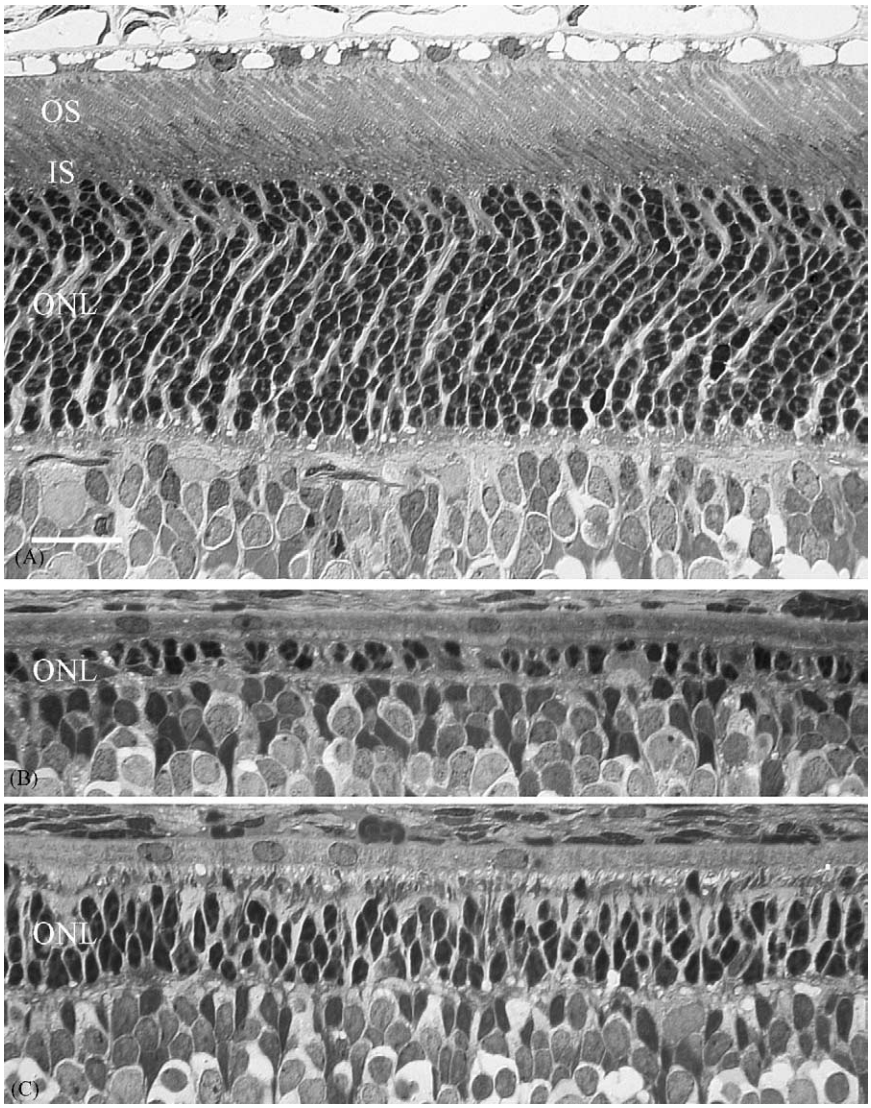

Fig. 7. Protection of photoreceptors in vivo by MITO-4565. Plastic-embedded sections of superior retinas from a normal (wild-type) rat (A), or retinas from 10 transgenic rats treated with vehicle in the right eye (DMSO) (B), or MITO-4565 in DMSO in the left eye (C) were examined at PD 20 by light microscopy. The normal retina has well developed outer and inner segments and the ONL has 11–12 rows of nuclei (A). In the vehicle treated retina of an S334ter-3 rat, the ONL has only 1–2 rows of nuclei and inner segments are very short stumps (B). In the left retina of the same animal treated with MITO-4565 (C), the ONL has 2–4 rows of nuclei. Sections were stained with toluidine blue. OS, outer segment; IS, inner segment; ONL, outer nuclear layer. Scale bar, 20 μm.

to rectify membrane peroxidation [57], a circumstance normally constrained by the relatively limited activity of the enzyme phospholipid hydroperoxide glutathione peroxidase [71]. This mechanism is directly analogous to tocopherol-ascorbate redox cycling, except that the redox potential for the ascorbate coupling is lower [72], and redox cycling of the phenolic steroids is dependent on availability of reduced glutathione, NADPH and the catalytic capacity of glutathione reductase, not availability of ascorbate and ascorbate reductase activities. Importantly, glutathione pools within the mitochondria are actively maintained at extraordinarily high concentrations, typically 8–10 mM [73]. In this way, potency of the phenolic steroids in vivo is largely dictated by the availability of reduced glutathione, which is extraordinarily high in most subcellular compartments, and by the kinetics of the reaction between GSH and the phenolic steroid, not by the antioxidant reactivity of the phenolic steroids per se, which are generally not exceptional [52,74].

If correct, this model predicts not only that the phenolic steroids should be more efficient moderators of lipid peroxidation in the presence of GSH, but also that the compounds should augment glutathione utilization under oxidative stress. Both predictions are supported by the data here.

In the first case, the cytoprotective phenolic steroids effectively moderate AMVN-induced hydroperoxide formation in phosphatidyl choline liposomes in vitro (Figs. 2 and 3A), whereas MITO-4555 and MITO-4567, neither of which are cytoprotective, are unable to do so (Table 1). Importantly, in concert with a cytoprotective compound, exogenous GSH substantially forestalls lipid peroxidation

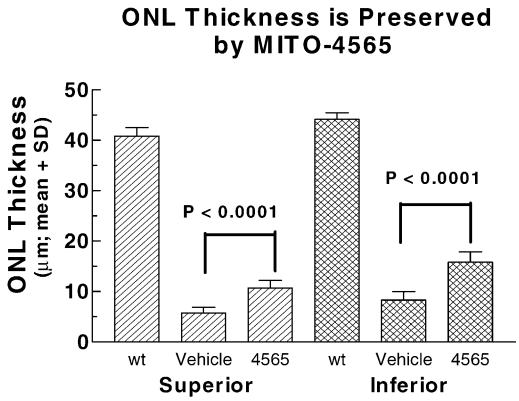

Fig. 8. Retinal protection by MITO-4565 shown in Fig. 7 was quantified by measuring the thickness of the ONL in both the superior and inferior retina after treatment of S334ter animals with MITO-4565. When measured on PD 20, a single injection of MITO-4565 on PD 9 almost doubles the thickness of the ONL compared to the vehicle-treated contralateral eye (ANOVA $F = 1100$, $P < 0.0001$, $N = 10$ for superior; $F = 696$, $P < 0.0001$, $N = 10$ for inferior). Note the almost 90% loss of photoreceptors by PD 20 in the vehicle treated S334ter eyes compared to wild-type controls.

formation in this model, and only after 130 min do the rate regressions converge (Fig. 3B), a likely reflection of declining GSH availability, and to some extent its reaction kinetics with the phenolic steroid. The experimental conditions in Fig. 3A and B were necessarily altered to accommodate differing kinetics and to focus on potential effects of GSH, but even the qualitative comparisons are sufficient to reveal involvement of GSH, as is also seen in the data in Table 1. Interestingly, α-tocopherol is a very potent inhibitor of peroxidation in this model, showing 98.6% (±1.7 S.E., $N = 3$) inhibition at the same 30 min time point presented in Table 1. However, between 86 and 100 min, the rate of peroxidation increases by over 25%, and continues to accelerate until the end of the experiment at 150 min, a likely reflection of α-tocopherol depletion and absence of ascorbate (data not shown).

The physical constraints of this micelle system likely serve to underestimate the actual efficiency of GSH-coupled redox cycling with the phenolic steroids. Because of their hydrophobicity, induction of peroxidation by AMVN, and the termination of peroxidation chain reactions by the phenolic steroid, occur throughout the solid multilamellar liposome. As such, these parameters are functions of the volume of the virtually solid microsome sphere. On the other hand, because of the hydrophilic nature of GSH, potential redox cycling between it and the oxidized phenolic steroid can occur only at the surface of the sphere exposed to the aqueous media. As a result, at any particle size with a radius greater than 3 μm, surface area-to-volume considerations impose an unavoidable limitation on redox cycling compared to induction of peroxidation. The micelles were plainly visible in suspension without magnification, indicating that the average size considerably exceeded 3 μm, which would correspondingly underestimate the relationship between internal peroxidation and redox cycling with the aqueous media at the surface.

In the second case, viz., that these compounds should augment glutathione redox cycling in vivo under oxidative stress, flux through the glycolytic HMS was monitored in intact human erythrocytes as an index of NADPH turnover, and hence GSH utilization. The latter linkage is tenable because of the metabolic simplicity of human RBCs, which lack a nucleus and mitochondria, thereby eliminating gene expression, protein synthesis, and the complex suite of oxidative metabolic pathways in mitochondria as confounding variables [60,61,63]. It should be noted that glutathione reductase is not the only oxidatively responsive enzyme in RBCs that requires NADPH as a cofactor; methemoglobin reductase, for example, is the other major source of NADPH turnover in RBCs [60,61]. However, the antioxidant activities of the phenolic steroids would serve to moderate methemoglobin formation, thereby reducing the confounding utilization of NADPH by methemoglobin reductase. In any event, it is apparent that HMS flux is increased in oxidatively stressed RBCs by those phenolic steroids with cytoprotective activities, whereas the non-cytoprotective compound fails to do so (Fig. 4B). The phenolic steroids do not alter HMS flux in the absence of an imposed oxidative load (Fig. 4A), suggesting not only that under unstressed conditions endogenous antioxidant mechanisms are adequate, but also that the molecules themselves are not perturbing metabolic or oxidative poise under such conditions. Although it is suggestive that MITO-4565, the most potent cytoprotectant examined, also elicited the greatest acceleration of HMS flux, data quantifying the extent of lipid peroxidation induced by H_2O_2 will be required before the stoichiometry between NADPH turnover and phenolic steroid potency, essentially the catalytic efficiency of the redox cycling, can be determined.

A membrane stabilization mechanism would be especially crucial to mitochondria, where function and failure, and hence cellular viability–necrosis–apoptosis, are closely tied to impermeability of the inner membrane and maintenance of $\Delta\Psi_m$ [57]. It bears reiteration in this context that mitochondrial glutathione levels are extraordinarily high, typically 8–10 mM, suggesting that protective phenolic steroids may be particularly effective at the level of the mitochondria. Indeed, in situ data from the FRET assay of $\Delta\Psi_m$ indicate that the cytoprotective molecules permit mitochondria to retain $\Delta\Psi_m$ under conditions that induce permeability transition in untreated mitochondria (Fig. 5). This is apparent in the right shift in the dose–response regressions to Ca^{2+}-induced mitochondrial collapse (Fig. 5), an effect also reflected by the EC_{50} values presented in Section 3, as well as by the preservation of adenylate status, repression of free radical production and moderation of apopotosis reported by others [2,36,50,75].

The cytoprotective phenolic steroids yield an average 28% increase in Ca^{2+} tolerance. Although this may seem a modest response, in terms of physiological function it

reflects that treatment with these compounds allows well over 50% the mitochondrial pool to retain $\Delta\Psi_m$ and function under Ca^{2+} loads sufficient to almost completely dissipate $\Delta\Psi_m$ in untreated mitochondria (Fig. 5). In this light, and given the physiological scope shown by most aerobically poised cells, 50% retention of mitochondrial function should translate into profound cytoprotection. Such cytoprotection is observed using retinal ganglion cells in primary culture, where NMDA excitotoxicity is significantly repressed by the parental estradiols and MITO-4565, but not by MITO-4567, the methoxy A-ring negative control (Fig. 6).

Mitochondrial protective therapeutic strategies ought to provide benefit in those ailments where apoptosis contributes to etiology. Since the loss of retinal photoreceptors in both human retinitis pigmentosa and the S334ter transgenic animal model of this disease is demonstrably due to an apoptotic pathway initiated by mitochondrial failure [16], the ability of MITO-4565 to moderate apoptosis in this model was assessed in vivo. A single injection of MITO-4565 into the left eye on postnatal day 9 significantly ($P < 0.0001$) moderates loss of photoreceptors in both the inferior and superior domains of the ONL in the S334ter rats compared to the vehicle-treated right eye (Figs. 7 and 8).

This dosing regime and experimental design are the same as those used to assess other treatments, thereby permitting comparisons. It is notable that the protective effect of the small molecule MITO-4565 is comparable to that obtained with cardiotropin 1 (CT-1) also given as a single injection on PD 9 [76]. CT-1, as well as ciliary neurotrophic factor (CNTF), are members of the IL-6 family of cytokines, which exhibit excellent photoreceptor protective effects over a broad range of models and species, including rat, mouse, and dog [16,65,77].

It seems likely that the intraocular route of administration used here in vivo would result in high exposures to MITO-4565; in the absence of protein binding, 2 μl of a 10 mM solution injected into approximately 20–30 μl vitreous humor would yield a concentration of ~1 mM, far in excess of effective doses in other in vitro and in vivo models. However, the parental estrogens are bound to serum proteins in vivo, and MITO-4565 may well be bound by proteins in the vitreous humor, which would lower the effective concentration at the retina. Moreover, on a more physiologically realistic scale, with each layer of the ONL composed of $\sim 1 \times 10^6$ photoreceptors and exposed to 1 mM compound, versus ~80,000 cells exposed to ~1–2.5 μM in the 96-well assay, the effective concentrations of compound per cell are not orders of magnitude different. Confirmation of this supposition awaits data from on-going studies of administration routes and subsequent tissue extractions for quantitative analysis. As an aside, although it would be instructive to examine the effects of multiple dosing, a second intraocular injection of MITO-4565 in DMSO was not well-tolerated.

Finally, although the data here support a mechanistic model of membrane stabilization and consequent retention of mitochondrial function, estrogens and other phenolic analogs demonstrate additional activities that also likely contribute to cytoprotection. For example, 17α-E2 represses potentially cytotoxic Ca^{2+} influx in several cell types [78], while both 17α-E2 and 17β-E2 increase cytosolic glucose concentrations, probably by moderating efflux at the GLUT 1 transporter [79,80]. Moreover, estrogens allosterically modulate the activity of several key metabolic regulatory enzymes, like glyceraldehyde-3-phosphate dehydrogenase [81] and, importantly, mitochondrial F_0F_1-ATP synthase, where the oligomycin sensitivity-conferring protein subunit has an estrogen-binding domain through which estrogen can directly modulate cellular energetic metabolism [82,83]. These and other non-genomic effects of phenolic steroids would also impinge on mitochondrial function, and hence on cytoprotection. For example, repression of Ca^{2+} influx would help forestall mitochondrial permeability transition, inhibition of ATP synthase would serve to preserve adenylate charge during hypoxia, and increased glucose availability would correspondingly increase glycolytic ATP production, as well as potential flux through HMS. The interdependence of metabolic pathways also yields more circuitous routes to mitochondrial protection; preservation of adenylate status by estrogens, via one or all of the above mechanisms, would serve to protect mitochondrial function because ATP is an extraordinarily potent stabilizer of mitochondrial integrity. These possibilities await further investigation with other novel phenolic steroids.

In the interim, it is increasingly apparent that therapeutic strategies targeting stabilization of mitochondrial function will yield benefits in diseases like retinitis pigmentosa, where apoptosis underlies etiology, and where therapies have been lacking. Indeed, it is also increasingly apparent that phenolic steroids, and other mitochondrial interventions, offer novel therapeutic avenues for other widespread degenerative diseases, including those of the central and peripheral nervous systems, as well as type II diabetes, which is associated with mitochondrial senescence in the pancreatic beta-cells [84–86], in osteoarthritis [87,88], and in a host of other diseases where mitochondrial dysfunction contributes to etiology [89,90].

Acknowledgements

This work was supported by a grant from the Foundation Fighting Blindness (RW) and grants from NIH NEI (EY 15422, JAD; EY 12727, RW). We thank Dr. Katherine Gordon for helping to launch this project, and Dr. James Simpkins at UNTHSC for their continuing insights into the mechanisms of action and utility of these molecules. We also thank Yun Liu for excellent technical assistance, and Margaret Dykens for editorial comments.

References

[1] Portera-Cailliau C, Sung C-H, Nathans J, Adler R. Apoptotic photoreceptor cell death in mouse models of retinitis pigmentosa. Proc Natl Acad Sci USA 1994;91:974–8.

[2] Green PS, Gridley KE, Simpkins JW. Nuclear estrogen receptor independent neuroprotection by estratrienes: a novel interaction with glutathionine. Neuroscience 1997;84:7–10.

[3] Dryja TD, McGee TL, Reichel E, Hohn LB, Cowley GS, Yandell DN, et al. A point mutation of the rhodopsin gene in one form of retinitis pigmentosa. Nature 1990;343:364–6.

[4] Dryja TP, McGee TL, Hahn LB, Cowley GS, Olsson JE, Reichel E, et al. Mutations within the rhodopsin gene in patients with autosomal dominant retinitis pigmentosa. N Engl J Med 1990;323:1302–7.

[5] Farrar GJ, McWilliam P, Bradley DG, Kenna P, Lawler M, Sharp EM, et al. Autosomal dominant retinitis pigmentosa: linkage to rhodopsin and evidence for genetic heterogeneity. Genomics 1990;8:35–40.

[6] Travis GH, Brennan MB, Danielson PE, Kozak CA, Sutcliffe JG. Identification of a photoreceptor-specific mRNA encoded by the gene responsible for retinal degeneration slow (rds). Nature 1989;338: 70–3.

[7] Farrar GJ, Kenna P, Jordan SA, Kumar-Singh R, Humphries MM, Sharp EM, et al. A three-base-pair deletion in the peripherin-RDS gene in one form of retinitis pigmentosa. Nature 1991;354:478–80.

[8] Kajiwara K, Hahn LB, Mukai S, Travis GH, Berson EL, Dryja TP. Mutations in the human retinal degeneration slow gene in autosomal dominant retinitis pigmentosa. Nature 1991;354:480–3.

[9] Bowes C, Li T, Danciger M, Baxter LC, Applebury ML, Farber DB. Retinal degeneration in the rd mouse is caused by a defect in the beta subunit of rod cGMP-phosphodiesterase. Nature 1989;347:677–80.

[10] McLaughlin ME, Ehrhart TL, Berson EL, Dryja TP. Mutation spectrum of the gene encoding the beta subunit of rod phosphodiesterase among patients with autosomal recessive retinitis pigmentosa. Proc Natl Acad Sci USA 1995;92:3249–53.

[11] McLaughlin ME, Sandberg MA, Berson EL, Dryja TP. Recessive mutations in the gene encoding the beta-subunit of rod phosphodiesterase in patients with retinitis pigmentosa. Nat Genet 1993;4:130–4.

[12] Kajiwara K, Berson EL, Dryja TP. Digenic retinitis pigmentosa due to mutations at the unlinked peripherin/RDS and ROM1 loci. Science 1994;264:1604–8.

[13] Olsson JE, Gordon JW, Pawlyk BS, Roof D, Hayes A, Molday RS, et al. Transgenic mice with a rhodopsin mutation (Pro23His): a mouse model of autosomal dominant retinitis pigmentosa. Neuron 1992;9:815–30.

[14] Steinberg RH, Flannery JG, Naash M, Oh P, Matthes MT, Yasumura D, et al. Trangenic rat models of inherited retinal degeneration caused by mutant opsin genes. Invest Ophthalmol Vis Sci 1996;37:698.

[15] Petters RM, Alexander CA, Wells KD, Collins EB, Sommer JR, Blanton MR, et al. Genetically engineered large animal model for studying cone photoreceptor survival and degeneration in retinitis pigmentosa. Nat Biotech 1997;15:965–70.

[16] Liu C, Li Y, Peng M, Laties AM, Wen R. Activation of caspase-3 in the retina of transgenic rats with the rhodopsin mutation S334ter during photoreceptor degeneration. J Neurosci 1999;19(12):4778–85.

[17] Chang GQ, Hao Y, Wong F. Apoptosis: final common pathway of photoreceptor death in rd, rds, and rhodopsin mutant mice. Neuron 1993;11:595–605.

[18] Davidson FF, Steller H. Blocking apoptosis prevents blindness in *Drosophila* retinal degeneration mutants. Nature 1998;391:587–91.

[19] Kurada P, O'Tousa JE. Retinal degeneration caused by dominant mutations in *Drosophila*. Neuron 1995;14:571–9.

[20] Steele F, O'Tousa JE. Rhodopsin activation causes retinal degeneration in *Drosophila* rdgC mutant. Neuron 1990;4:883–90.

[21] Tatton NA, Tezel G, Insolia SA, Nandor SA, Edward PD, Wax MB. In situ detection of apoptosis in normal pressure glaucoma. A preliminary examination. Surv Ophthalmol 2001;45(Suppl. 3):S268–72.

[22] Lemasters JJ, Qian T, Bradham CA, Brenner DA, Cascio WE, Trost LC, et al. Mitochondrial dysfunction in the pathogenesis of necrotic and apoptotic cell death. J Bioenerg Biomembr 1999;31:305–19.

[23] Kroemer G, Reed JC. Mitochondrial control of cell death. Nat Med 2000;6:513–9.

[24] Kim JS, He L, Lemasters JJ. Mitochondrial permeability transition: a common pathway to necrosis and apoptosis. Biochem Biophys Res Commun 2003;304:463–70.

[25] Ferri KF, Kroemer G. Organelle-specific initiation of cell death pathways. Nat Cell Biol 2001;3:E255–63.

[26] Dykens JA, Stern A, Trenkner E. Mechanism of kainate toxicity to cerebellar neurons in vitro is analogous to reperfusion tissue injury. J Neurochem 1987;49:1222–8.

[27] Dykens JA. Mitochondrial free radical production and the etiology of neurodegenerative disease. In: Beal MF, Bodis-Wollner I, Howell N, editors. Neurodegenerative diseases: mitochondria and free radicals in pathogenesis. John Wiley & Sons; 1997. p. 29–55.

[28] Murphy AN, Fiskum G, Beal MF. Mitochondria in neurodegeneration: bioenergetic function in cell life and death. J Cereb Blood Flow Metab 1999;19:231–45.

[29] Bloss TA, Witze ES, Rothman JH. Suppression of CED-3-independent apoptosis by mitochondrial betaNAC in *Caenorhabditis elegans*. Nature 2003;424:1066–71.

[30] Halestrap AP. The mitochondrial permeability transition: its molecular mechanism and role in reperfusion injury. Biochem Soc Symp 1999;66:181–203.

[31] Dykens JA. Free radicals and mitochondrial dysfunction in excitotoxicity and neurodegenerative diseases. In: Koliatos VE, Ratan RR, editors. Cell death and diseases of the nervous system. New Jersey: Humana Press; 1999. p. 45–68.

[32] Andreyev A, Fiskum G. Calcium induced release of mitochondrial cytochrome c by different mechanisms selective for brain versus liver. Cell Death Differ 1999;6:825–32.

[33] Nickells RW. Apoptosis of retinal ganglion cells in glaucoma: an update of the molecular pathways involved in cell death. Surv Ophthalmol 1999;43:151–61.

[34] Lee SJ, McEwen BS. Neurotropic and neuroprotective actions of estrogens and their therapeutic implications. Annu Rev Pharmacol Toxicol 2001;41:569–91.

[35] Yu X, Rajala RVS, McGinnis JF, Li F, Anderson RE, Yan X, et al. Involvement of insulin/PI3K/Akt signal pathway in 17β-estradiol-mediated neuroprotection. J Biol Chem (e-published Jan 9, 2004).

[36] Bishop J, Simpkins JW. Estradiol treatment increases viability of glioma and neuroblastoma cells in vitro. Mol Cell Neurosci 1994;5:303–8.

[37] Green PS, Bishop J, Simpkins JW. 17α-estradiol exerts neuroprotective effects in SK-N-SH cells. J Neurosci 1997;17:511–5.

[38] Goodman Y, Bruce AJ, Cheng B, Mattson MP. Estrogens attenuate and corticosterone exacerbates excitotoxicity, oxidative injury, and amyloid b-peptide toxicity in hippocampal neurons. J Neurochem 1996;66:1836–44.

[39] Pike C. Estrogen modulates neuronal Bcl-xl expression and b-amyloid-induced apoptosis: relevance to Alzheimer's disease. J Neurochem 1999;72:1552–63.

[40] Behl C, Skutella T, Lezoualch F, Post A, Widmann M, Newton CJ, et al. Neuroprotection against oxidative stress by estrogens: structure–activity relationship. Mol Pharmacol 1997;51:535–41.

[41] Sawada H, Ibi M, Kihara T, Urushitani M, Akaike A, Shimohama S. Estradiol protects mesencephalic dopaminergic neurons from oxidative stress-induced neuronal death. J Neurosci Res 1998;54:707–19.

[42] Green PS, Simpkins JW. Neuroprotective effects of estrogens: potential mechanism of action. Int J Dev Neurosci 2000;18:347–58.

[43] Garcia-Segura LM, Azcoitia I, DonCarlos LL. Neuroprotection by estradiol. Prog Neurobiol 2001;63:29–60.

[44] Nonaka A, Kiryu J, Tsujikawa A, Wamashiro K, Miyamoto K, Nishiwaki H, et al. Administration of 17β-estradiol attenuates retinal

ischemia-reperfusion injury in rats. Invest Ophthalmol Vis Sci 2000;41:2689–96.
[45] Simpkins JW, Rajakumar G, Zhang Y-Q, Simpkins C, Greenwald D, Yt CJ, et al. Estrogens may reduce mortality and ischemic damage caused by middle cerebral artery occlusion in the female rat. J Neurosurg 1997;87:724–30.
[46] Dubal DB, Kashon ML, Pettigrew LC, Ren JM, Finklestein SP, Rau SW, et al. Estradiol protects against ischemic injury. J Cereb Blood Flow Metab 1998;18:1253–8.
[47] Yang SH, Shi J, Day AL, Simpkins JW. Estradiol exerts neuroprotective effects when administered after ischemic insult. Stroke 2000;31:745–9.
[48] Fan T, Yang SH, Johnson E, Osteen B, Hayes R, Day AL, et al. 17beta-Estradiol extends ischemic thresholds and exerts neuroprotective effects in cerebral subcortex against transient focal cerebral ischemia in rats. Brain Res 2003;993:10–7.
[49] Azcoitia I, Sierra AM, Garcia-Segura LM. Estradiol prevents kainic acid-induced neuronal loss in the rat dentate gyrus. Neuroreport 1998;9:3075–9.
[50] Nakamizo T, Urushitani M, Inoue R, Shinohara A, Sawada H, Honda K, et al. Protection of cultured spinal motor neurons by estradiol. Neuroreport 2000;11:3493–7.
[51] Green PS, Gordon K, Simpkins JW. Phenolic A ring requirement for the neuroprotective effects of steroids. J Steroid Biochem Mol Biol 1997;63:229–35.
[52] Green PS, Yang SH, Nilsson KR, Kumar AS, Covey DF, Simpkins JW. The nonfeminizing enantiomer of 17beta-estradiol exerts protective effects in neuronal cultures and a rat model of cerebral ischemia. Endocrinology 2001;142:400–6.
[53] Moosmann B, Behl C. The antioxidant neuroprotective effects of estrogens and phenolic compounds are independent from their estrogenic properties. Proc Natl Acad Sci USA 1999;92:9692–6.
[54] Dicko A, Morissette M, Ben Ameur S, Pezolet M, Di Paolo T. Effect of estradiol and tamoxifen on brain membranes: investigation by infrared and fluorescences pectroscopy. Brain Res Bull 1999;49: 401–5.
[55] Levin LA, Clark JA, Johns LK. Effect of lipid peroxidation inhibition on retinal ganglion cell death. Invest Ophthalmol Vis Sci 1996; 37:2744–9.
[56] Liang Y, Belford S, Tang F, Prokai L, Simpkins JW, Hughes JA. Membrane fluidity effects of estratrienes. Brain Res Bull 2001; 54:661–8.
[57] Xia S, Cai ZY, Thio LL, Kim-Han JS, Dugan LL, Covey DF, et al. The estrogen receptor is not essential for all estrogen neuroprotection: new evidence from a new analog. Neurobiol Dis 2002;9:282–93.
[58] Dykens JA, Simpkins JW, Wang J, Gordon K. Polyphenolic steroids and neuroprotection: a proposed mitochondrial mechanism. Exp Gerontol 2003;38:101–7.
[59] Dykens JA. Isolated cerebellar and cerebral mitochondria produce free radicals when exposed to elevated Ca^{2+} and Na^{+}: implications for neurodegeneration. J Neurochem 1994;63:584–91.
[60] Liu R, Yang SH, Perez E, Yi KD, Wu SS, Eberst K, et al. Neuroprotective effects of a novel non-receptor-binding estrogen analogue: in vitro and in vivo analysis. Stroke 2002;33:2485–91.
[61] Trotta RJ, Sullivan SG, Stern A. Lipid peroxidation and haemoglobin degradation in red blood cells exposed to *t*-butyl hydroperoxide. Effects of the hexose monophosphate shunt as mediated by glutathione and ascorbate. Biochem J 1982;204:405–15.
[62] Dykens JA, Sullivan SG, Stern A. The red cell as a model for drug-induced oxidant stress. In: Rice-Evans C, editor. Free radicals oxidant stress and drug action. London: Richelieu Press; 1987. p. 31–4.
[63] Dykens JA, Stout AK. Fluorescent dyes and assessment of mitochondrial membrane potential in FRET modes. Methods Cell Biol 2001;65:285–309.
[64] Dykens JA, Sullivan SG, Stern A. Glucose metabolism and hemoglobin reactivity in human red blood cells exposed to tryptophan metabolites from the kynurenine pathway. Biochem Pharmacol 1989;38:1555–62.
[65] Dykens JA, Fleck B, Ghosh S, Lewis M, Velicelebi G, Ward M. A novel FRET-based assay of mitochondrial membrane potential in situ. Mitochondrion 2002;1:461–73.
[66] LaVail MM, Unoki K, Yasumura D, et al. Multiple growth factors, cytokines, and neurotrophins rescue photoreceptors from the damaging effects of constant light. Proc Natl Acad Sci USA 1992; 89:11249.
[67] LaVail MM, Yasumura D, Matthes MT, et al. Protection of mouse photoreceptors by survival factors in retinal degenerations. Invest Ophthalmol Vis Sci 1998;39:592.
[68] Chernayaev GA, Barkova TI, Egorova VV, Sorokina IB, Ananchenko SN, Mataradze GD, et al. A series of optical, structural and isomeric analogs of estradiol: a comparative study of the biological activity and affinity to cytosol receptor of rabbit uterus. J Ster Biochem 1975; 6:1483–8.
[69] Payne DW, Katzenellenbogen JA. Binding specificity of rat a-fetoprotein for a series of estrogen derivatives: studies using equilibrium and nonequilibrium binding techniques. Endocrinology 1979;105: 743–53.
[70] Terenius L. Differential inhibition in vitro of 17b-estradiol binding in the mouse uterus and vagina by optical antipodes of estrogens. Mol Pharmacol 1968;4:301–10.
[71] Blum-Degen D, Haas M, Pohli S, Harth R, Romer W, Oettel M, et al. Scavestrogens protect IMR 32 cells from oxidative stress-induced cell death. Toxicol Appl Pharmacol 1998;152:49–55.
[72] Zhao L, Wang HP, Zhang HJ, Weydert CJ, Domann FE, Oberley LW, et al. L-PhGPx expression can be suppressed by antisense oligodeoxynucleotides. Arch Biochem Biophys 2003;417:212–8.
[73] Buettner GR. The pecking order of free radicals and antioxidants: lipid peroxidation, alpha-tocopherol, and ascorbate. Arch Biochem Biophys 1993;300:535–43.
[74] Meredith MJ, Reed DJ. Status of the mitochondrial pool of glutathione in the isolated hepatocyte. J Biol Chem 1982;257:3747–53.
[75] Bhavnani BR, Cecutti A, Gerulath A, Woolever AC, Berco M. Comparison of the antioxidant effects of equine estrogens, red wine components, vitamin E, and probucol on low-density lipoprotein oxidation in postmenopausal women. Menopause 2001;8:395–7.
[76] Wang J, Green PS, Simpkins JW. Estradiol protects against ATP depletion, mitochondrial membrane potential decline and the generation of reactive oxygen species induced by 3-nitropropionic acid in SK-N-SH human neuroblastoma cells. J Neurochem 2001;77:804–11.
[77] Song Y, Zhao L, Tao W, Laties AM, Luo Z, Wen R. Photoreceptor protection by cardiotrophin-1 in transgenic rats with the rhodopsin mutation S334ter. Invest Ophthalmol Vis Sci 2003;44:4069–75.
[78] Tao W, Wen R, Goddard MB, Sherman SD, O'Rourke PJ, Stabila PF, et al. Encapsulated cell based delivery of CNTF reduces photoreceptor degeneration in animal models of retinitis pigmentosa. Invest Ophthalmol Vis Sci 2002;43:3292–8.
[79] Seeger H, Mueck AO, Oettel M, Schwarz S, Lippert TH. Calcium antagonistic effect of 17α-estradiol derivatives: in vitro examinations. Gynecol Endocrinol 1999;13:246–8.
[80] Fraser H, Davidge ST, Clanachan AS. Enhancement of post-ischemic myocardial function by chronic 17beta-estradiol treatment: role of alterations in glucose metabolism. J Mol Cell Cardiol 1999;31: 1539–49.
[81] Afzel I, Cunningham P, Naftalin RJ. Interactions of ATP, oestradiol, genistein and the anit-oestrogens, faslodex (ICI 182780) and tamoxifen, with the human erythrocyte glucose transporter GLUT 1. Biochem J 2002;365(Pt. 3):707–19.
[82] Ramirez VD, Kipp JL, Joe I. Estradiol, in the CNS, targets several physiologically relevant membrane-associated proteins. Brain Res Rev 2001;37:141–52.
[83] Zhang J, Ramirez VD. Purification and identification of an estrogen binding protein from rat brain: oligomycin sensitivity-conferring

protein (OSCP), a subunit of mitochondrial F0F1-ATP aynthase/ ATPase. J Steroid Biochem Mol Biol 1999;68:65–75.

[84] Zhang J, Ramirez VD. Rapid inhibition of rat brain mitochondrial proton F0F1-ATPase activity by estrogens: comparison with Na^+/K^+-ATPase of porcine cortex. Eur J Pharmacol 1999;368:95–102.

[85] Maechler P, Wollheim CB. Mitochondrial function in normal and diabetic β-cells. Nature 2001;414:807–12.

[86] Lee B, Miles PD, Vargas L, Luan P, Glasco S, Kushnareva Y, et al. Inhibition of mitochondrial Na^+–Ca^{2+} exchanger increases mitochondrial metabolism and potentiates glucose-stimulated insulin secretion in rat pancreatic islets. Diabetes 2003;52:965–73.

[87] Anderson CM. Mitochondrial dysfunction in diabetes mellitus. Drug Dev Res 1999;46:67–79.

[88] Johnson K, Jung A, Murphy A, Andreyev A, Dykens J, Terkeltaub R. Mitochondrial oxidative phosphorylation is a downstream regulator of nitric oxide effects on chondrocyte matrix synthesis and mineralization. Arthritis Rheum 2000;43:1560–70.

[89] Terkeltaub R, Johnson K, Murphy A, Ghosh S. Invited review: the mitochondrion in osteoarthristis. Mitochondrion 2002;1:301–19.

[90] Dykens JA. Mitochondrial radical production and mechanisms of oxidative excitotoxicity. In: Davies KJA, Ursini F, editors. The oxygen paradox. U. of Padova: Cleup Press; 1995. p. 453–67.